

# Intensity Profile Measurement for Carbon Steel Pipe using Gamma-Ray Tomography

Susiapan, Y.S.<sup>1</sup> Ruzairi, A. R.<sup>2, 3\*</sup>, Goh, C.L.<sup>2</sup> Hafiz, F. R.<sup>4</sup>, Herlina, A. R<sup>2</sup>

1 Faculty of Computing, Engineering & Technology (FCET) Asia Pacific University of Technology and Innovation (APU), MALAYSIA.

2 Faculty of Electrical Engineering Universiti Teknologi Malaysia, Skudai, Johor, 81310, MALAYSIA.

3 Faculty of Electrical and Electronic Engineering Universiti Tun Hussein Onn, Batu Pahat, Johor, 86400, MALAYSIA.

4 School of Mechatronic Engineering Universiti Malaysia Perlis, Arau, Perlis, 02600, MALAYSIA.

Received 24 January 2017; accepted 10 April 2017, available online 11 April 2017

**Abstract:** This paper details a non-destructive type of tomographic technique to obtain the intensity profile of a carbon steel pipe. This method requires a radioactive source, where a detector-source pair is mounted on a circular gantry located around the periphery of a steel pipe. A radioactive source with an appropriate activity was chosen based on the thickness of the pipe under test. In order to detect gamma rays, photon scintillation detectors are required. A Thallium-activated Sodium Iodide (NaI(Tl)) detector crystal was used. Stability tests were conducted on the detectors before they were ready to be used. A portable hardware to house the detector and source was then designed and built. For testing purposes, objects (polypropylene log, wax log, hollow polypropylene log, concrete log). The system was able to achieve an average accuracy of 96.283% when a comparison was done between actual dimension of the objects under test and the dimension based on the intensity profiles

**Keywords:** Gamma-ray Tomography; intensity profile; corrosion

## 1. Introduction

The word “tomography” is derived from the Greek language. “Tomo” means cutting section and “Graph” means image. Putting the two words together, we derive the idea that tomography is a field of science that is related to obtaining cross-sectional images of an object (Williams and Beck, 1996). Tomographic imaging provides the possibility of extracting information about a certain structure without physically invading or cutting into the object. Multiple projections taken at various views or angle around the object of test are used to generate data sets. These data are then processed usually using computer-based methodologies to reconstruct images that reflect the internal contents of the pipeline or process vessel under test (Dyakowski and Jaworski, 2003).

Industrial insulation is common to all industries that are dealing with flowing liquids, gases or solids. There are many integrity and safety challenges that have to be dealt with where industrial insulation is concerned. Corrosion, one of the more serious

issues, is one that requires urgent attention. Over time, pipes may corrode while set inside the insulation. Since these pipes are shielded from view, any sort of corrosion that occurs often goes unnoticed. These pipes often carry high-pressure, high-temperature gases, oils, hydrocarbons and many other highly dangerous and corrosive chemicals that are used in the processes specific to the industry. An example of this would be a petrochemical plant. The implication of corrosion on these critical pipes is insurmountable. Corrosion causes pipe deterioration, leading to damage resulting in leakages. These leakages often cause fires, massive explosions and fatalities.

Visual strip and search is a method used to detect corrosion. It is used widespread in the industry and is the only guaranteed method of detecting corrosion (Twomey, 1997). The insulation is first physically stripped off the pipe, allowing the pipe to be examined, and then the insulation is re-fitted. The visual strip and search method is generally carried out over a five-year period. On average, moisture or/and corrosion is often found in 5-20% of

inspected pipe. Thus, 80-95% need not be stripped in the first place as the integrity and condition of the pipe is often found to be sound. This method is an industry headache and massive resource drain. Annually, the National Association of Corrosion Engineers estimates losses due to corrosion, repairs and production downtime cost manufacturing industries in the USA to be around US\$17.6 billion. Figure 1 shows the distribution of corrosion related cases per year from 1959 until 2009 (Wood, 2010).

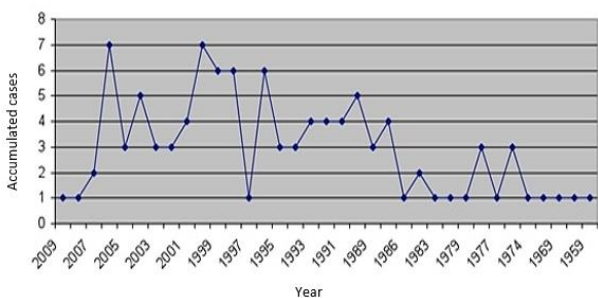


Figure 1: Corrosion related cases from 1959-2009.

Corrosion is insidious. It is not a new problem. It is in fact a well-understood problem, having been the bane of production pipelines for many years. Therefore, well-established inspection programs and mitigation methods have been in place for years. However, it is a problem that is persistent and stubbornly continues to force process industries to spend millions annually for repairs and downtime due to failure. According to the current U.S. corrosion study, the direct cost of metallic corrosion is \$276 billion on an annual basis. The average annual corrosion-related cost is estimated at \$7 billion to monitor, replace, and maintain these assets (Koch, et al., 2001). Corrosion is so prevalent and takes so many forms that its occurrence and associated costs cannot be eliminated completely. The bottom line is that the use of appropriate corrosion prevention and control methods protects public safety, prevents damage to property and the environment, and saves billions.

In order to detect defects for a carbon steel pipe, a portable gamma-ray tomography

instrumentation has been designed and developed. A basic tomography system consists of transmitter-detector pairs placed externally around the circumference of an object. The output signal from the sensors is then sent to a computer wirelessly or via an interface card to be logged. After the signal from the sensors has been received and logged, the computer can then proceed to the next phase of the process, the data processing, after which, a cross-sectional image of the pipe is constructed. In below sections, we discuss on the system designs, the testing procedures, the experiments and the results.

## 2. System Description

The principle of gamma-ray tomography measurement is based on the absorption of gamma radiation in the tested material. The scanning is performed using a small radioactive source and a sensitive electronic detector. The type and activity of the source depends on the thickness of the pipeline under test. A thicker pipeline would require a source having higher activity, determined via trial and error testing. A suitable source is one that is able to transmit its rays through and through but still retain sufficient information about the pipeline traversed. The detector used was a Thallium-activated Sodium Iodide (NaI(Tl)) detector crystal. Stability tests have to be conducted on the detectors before they are ready to be used.

The source and detector are kept external to the pipe and positioned on opposite sides at a fixed distance apart. Gamma rays travel from the source through the pipe to the detector where they are counted. A detector records the transmitted radiation and the measurement is then stored as an intensity profile.

A stability test, also known as an instrument voltage plateau test, is one of the quality control procedures for detectors that is conducted by end users. This test must be conducted before a scintillation detector can be used in order to obtain its most suitable operating voltage, at which point its readings are stable and dependable.

The collected data in the form of intensity is logged into an excel sheet and input in

offline mode to produce the intensity profile. The block diagram of the developed gamma-ray tomography system is shown in Figure 2.

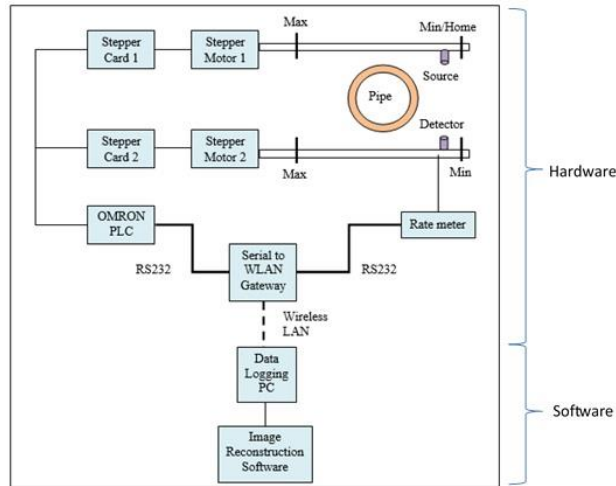


Figure 2: CUI tomographic system.

### 2.1 Mechanical Structure

This project deals with two stages of tomogram construction. The first stage consists of projection data sets being collected in parallel beam projection method. In the parallel beam projection technique, all measurements in a single set are taken along parallel paths. The projection measurements can be grouped in sets of parallel rays. After the first set is complete, the source-detector pair is then shifted along the circumference of the pipeline and the data collection is repeated in parallel with the diameter of the pipeline's cross-section at that position as shown in Figure 3. This is repeated until the entire circumference of the pipe under test is measured. The combination of two measurement modalities ensures complete coverage and maximizes sensor field view with minimum source-detector pairs required.

Figures 3, 4 and 5 illustrate the initial mechanical gantry constructed to house the detector and source, and for pipe placement. The source and detector are positioned at opposite ends of the pipe under test and then are moved simultaneously in parallel using stepper motors at precise distances as preset by the PLC. The maximum range of movement for the detector and source is 0-500 mm. As such, the maximum outer diameter of the pipe that can be tested by this system is

500 mm. The 'tracks' on which the source and detector move on are parallel to each other and can be set up to either move along the x-axis or y-axis. Using this setup, two projection sets are taken, one along the x-axis and another along the y-axis.

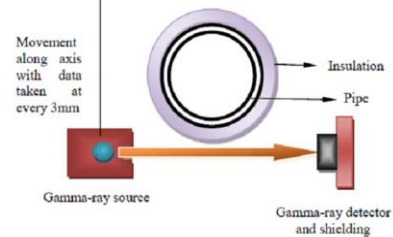


Figure 3: Mechanical gantry.

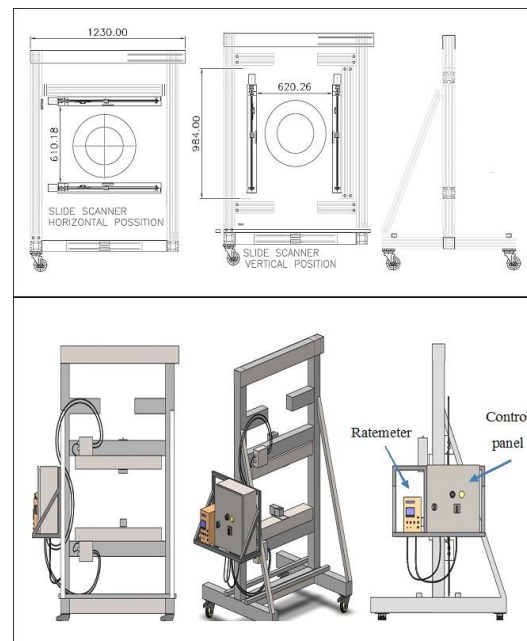


Figure 4: Portable design of mechanical structure.

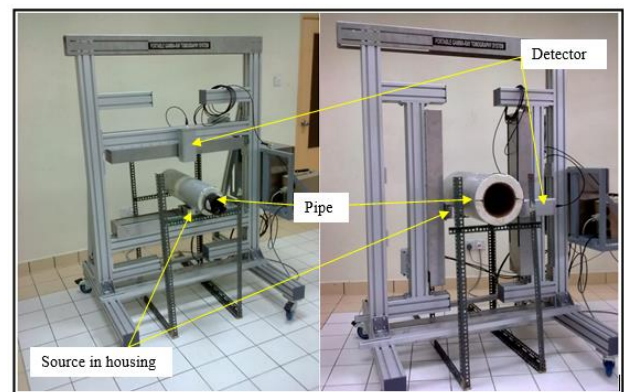


Figure 5: Detector Movement along x-axis and y-axis.

The setup described above allows only two projections, one along the x-axis and one along the y-axis. However, two projections are insufficient to correctly reflect the pipeline condition due to the asymmetrical, random formation of corrosion. To allow rotation around the pipe under test, a movable circular gantry was placed between the parallel beams. The rotating mechanism can be shifted by specific angular degrees depending on the size of the pipeline. The larger the diameter of the pipeline, the smaller the permissible angle of rotation. The mechanical system moves the source and the detector for a parallel beam scanning, and then rotates the gantry at a new projection angle for the next data set. The parallel structure and rotational movement is shown in Figures 6, 7 and 8. The red arrows represent the transmitted rays from the source to detector.

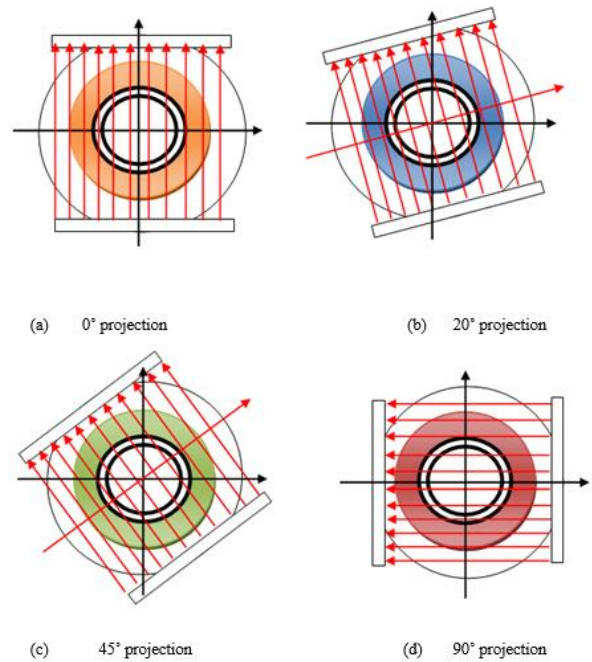
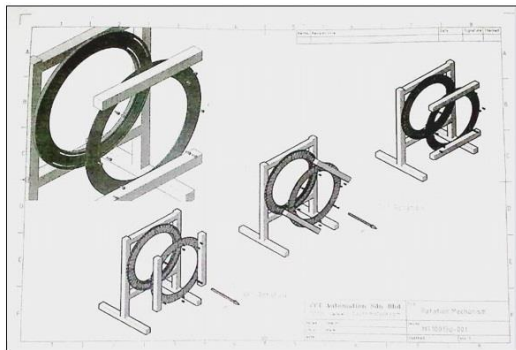
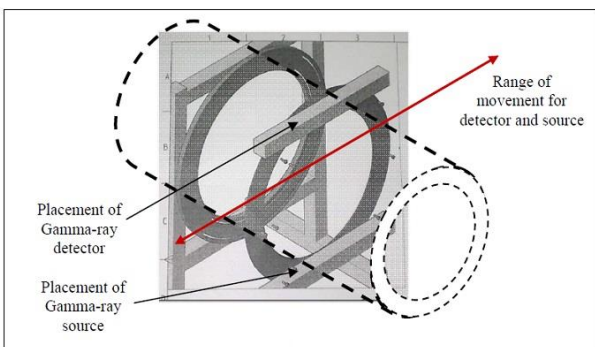


Figure 7 (a-d): Rotating mechanism at different projection angles



(a)



(b)

Figure 6(a, b): Rotating mechanism.

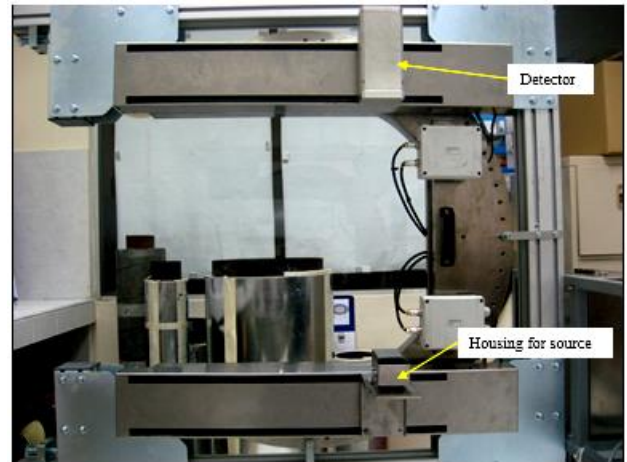


Figure 8: Front view of system with circular gantry

## 2.2 Source and Detector

The source selection and specification is dependent on several factors such as activity, source dimension, and energy. It should also emit radiation uniformly (Kim et al., 2011). From these conditions, a cylindrical source and a scintillation detector are preferred for the implementation of this project. Pipeline thickness is the deciding factor for the source energy since gamma-ray transmission increases with increasing gamma-ray energy and decreases with increasing absorber

thickness (G. Nelson and D. Reilly, 1991; McAlister, 2013). The source collimator restricts the spread of the radiation to a single narrow beam that traverses continuously across the pipe and hit the detector at the other end. Counts for the entire energy spectrum of the source chosen were considered during data acquisition and not only at the source's photo peak, which might have contributed to the fluctuations that resulted. Table 1 provides the specification of the sources and the detector used in our developed system. The half-life of an isotope refers to the time taken for the radioactivity of a specified isotope to fall to half its original value. The energy of the radiation is responsible for its ability to penetrate matter. Higher energy radiation can penetrate higher density matter and penetrate more than low energy radiation. The energy of ionizing radiation is measured in electronvolts (eV). The strength of a radioactive source is called its activity, which is defined as the rate at which the isotope decays.

Table 1 Source and Detector specifications.

Source (s)		Detector
Ba-133	Half-life - 10.51 years Energy - 80 keV Activity - 3.17 mCi	Thallium doped Sodium Iodide crystal material - NaI(Tl)
Cs-137	Half-life - 30.17 years Energy - 662 keV Activity - 2.81 mCi	

Minimising the number of sources required to be brought to the test site is preferred to ensure ALARP (As Low As Reasonable Possible) compliance. Therefore the developed system uses a single source-single, detector sensor array in a combination of first and second generation measurement geometry to keep exposure levels for personnel as low as reasonably possible but at the same time to maximise sensor field view.

### 3. Experiments and Results

In this section, results for the real-time construction of pipe profile for three pipe samples with various simulated defects are presented. The stability test was done to determine the most suitable operating voltage range for a scintillation detector. Finally a comparison between a good, clean carbon steel pipeline and a defective carbon steel pipeline is discussed.

#### 3.1 Stability Test for NaI(Tl) Scintillation Detector

Quality control and quality assurance procedures on nuclear instruments are a very necessary requirement to ensure that the instruments in question are safe for use, in good working order to ensure proper behaviour, and to reduce occurrences of false alarm pulses from interference, noise, high voltage failures and leaks. It is also a very important aspect to consider because in most cases, these instruments are related to personnel and national safety, radiological protection and critical industrial processes. Accurate representation and measurement of radiation quantities must be guaranteed to a high degree. Quality control tests are done at various levels starting at the manufacturers of the instruments right up to the end users.

Stability tests, also known as the instrument voltage plateau test, is one of the quality control procedures for detectors conducted by end users. This test must be conducted before a scintillation detector can be used in order to obtain its most suitable operating voltage, at which point its readings are stable and dependable

A scintillator is a material that exhibits scintillation, which is the property of luminescence when excited by ionizing radiation. By measuring the light emission from the scintillator, it is possible to detect ionizing radiation. However, the resultant light from scintillation is very low. Therefore, a few photons are converted into a usable, measureable electrical signal by the

photomultipliers and semiconductors. Figure 9 shows the NaI(Tl) scintillation detector used.



Figure 9: A scintillation detector.

Ratemeter, blocks of lead for shielding, checksource (Cs-137), and three detectors (named Detectors A, B, D) were the instruments to conduct experimental tests. The instruments required for the safety of the facility and the personnel are the film badge, gloves and surveymeter. Film badges or thermoluminescent dosimeters (TLDs) must be worn by all persons entering a site which houses radioactive materials. Gloves must be used when handling the lead blocks used for shielding to reduce risk of lead poisoning. A surveymeter must be used to monitor the surrounding radiation and ensure it is at safe levels whenever a radiation source is in the vicinity or in use. The ratemeter, checksource, detector and placement of the shielding are set up as shown in Figure 10.



Figure 10 : Stability test setup

The 'High Voltage Dial' or HV on the ratemeter is a 10-turn potentiometer control for adjusting HV from 200 V to 2500 V. It provides a linear adjustment of the detector voltage supply. Changing the detector voltage will cause the detector gain to change. A linear

change in voltage will cause an exponential change in detector gain. The instrument will support 100 megohm scintillation loads to 1500 V. The ratemeter 'Threshold' dial was set to '1'. The ratemeter multiplier set to 'x.1' and the numerical value set to '1' so that a reading is taken every 6 seconds for instance,  $0.1 \times 1 \text{ min.} = 6 \text{ seconds.}$

The HV dial setting adjusts detector gain and its setting is unique for different detectors. The most appropriate setting is determined from the plot of intensity counts versus voltage (system gain). If the HV dial setting is set to a value that is too high above or too low below its stable range, the intensity counts obtained may not be accurate or even usable. A HV setting that gives an intensity count of more than 6000 may result in the detector being damaged hence the test is stopped once the intensity count logged is approximately 5000 counts. In order to count the intensity, the ratemeter's HV Dial Setting was set to 1.5 and the 'count' button was pressed. The ratemeter 'HV Dial Setting' was gradually increased by 0.01 and the intensity counts were noted down until it was approximately 5000 counts. The optimum operating point for low background detectors is just above the inflection point (or break-over point) of the instrument plateau curve. Since the background count was irrelevant, the operating point was shifted to the plateau center for greater stability.

### 3.1.1 Stability Test Results

Intensity counts were measured using three detectors, namely Detectors A, B and D. Then, they were constructed into the graphs as shown in Figures 11, 12 and 13.

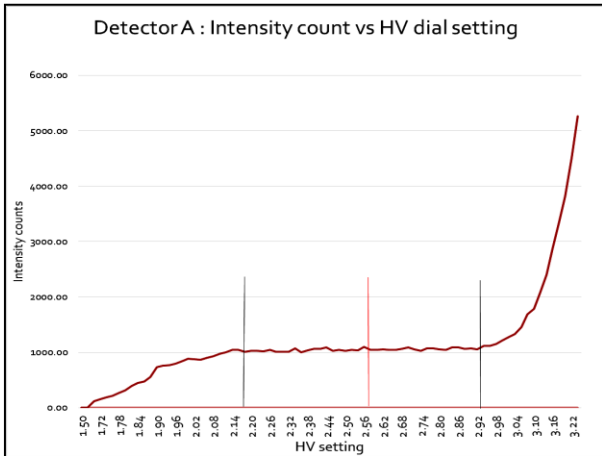


Figure 11: Intensity counts for Detector A.

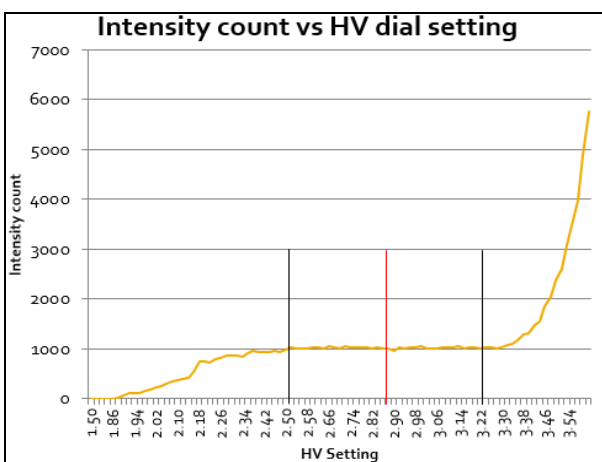


Figure 12: Intensity counts for Detector B.

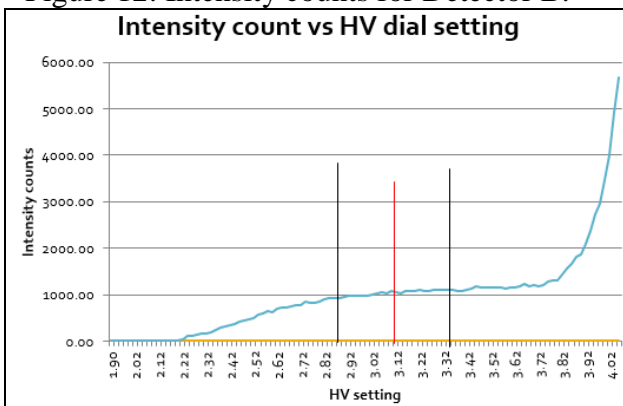


Figure 13: Intensity counts for Detector D.

The optimum HV dial setting is approximately midway between the two vertical black lines drawn on the graph. From the graphs, the most suitable HV settings for each detector, shown using red lines in Figures 11, 12 and 13, are found to be:-

- Detector A – 2.60 kV
- Detector B – 2.86 kV
- Detector D – 3.20 kV

### 3.2 Chi-Square Test

The Chi-Square test is a type of quality control test that demonstrates the soundness of the measurements made. It points to appropriate operation of the counting system when random pulses from a radioactive source are applied. As stated in IAEA-TECDOC-602 (1988), Chi-Square test results should be within 3.325 and 16.919. Results within these stated boundaries indicate that there are no instabilities in HV, amplifier, counters or any electronic influence. The chi square test is only dependent on the statistic pattern coming from a radioactive source.

The Chi Square method was performed on the previously determined HV settings for each detector (Detector A – 2.60 kV, Detector B – 2.86 kV, Detector D – 3.20 kV) and the results for the p-value are shown in Table 2.

Table 2 Chi square test results.

Detector	C <sub>i</sub>	C <sub>i</sub> average	$\sum(C_i - C_{iaverage})^2$	Chi Square
Detector D	3758	3816.67	33484.66	8.77
	3965			
	3727			
Detector B	1012	967.67	3428.66	3.54
	930			
	961			
Detector A	1044	1040	5226.00	5.02
	987			
	1089			

The chi-square values obtained for each HV setting fell in the valid range hence it can be concluded that these HV values obtained experimentally for each respective detector was its most suitable operating voltage, at which point readings obtained were stable and dependable. This is due to the condition that if the HV dial setting is set to a value that is too high above or too low below its stable range, the intensity counts obtained may not be accurate or even usable.

### 3.2.1 Experiments for Pipe Profile

#### 3.2.1.1 Accuracy of Profile Measurement

In order to evaluate the accuracy of the profile construction, the instrumentation described previously was tested and the data used to reconstruct the profile of a clean pipe and referenced with pipe using intentionally placed defects such as obstacles inside the pipeline and also under the insulation. These were the phantoms in this experiment. These objects had different dimensions and densities. The cross-section of a pipe along the x-axis and the y-axis was measured using gamma-ray and the physical characteristics of the pipe were verified based on the results. This evaluation of reconstruction algorithms for on-line measurement data is necessary in order to make general conclusions about their performances.

Besides the portable gamma-ray instrumentation, the tools for this were the two samples of insulated clean carbon steel pipes (Sample A, B), aluminum, scintillation detector (Detector A), radioactive source (Barium-133, 3.17mCi), polypropylene log, wax log, hollow polypropylene log, concrete log, ratemeter, caliper and measuring tape. Different obstacles were inserted into Sample A and B and measured using the instrumentation. Data was tabulated and used to graph the pipe profile. The specification of the samples, obstacles and the instrumentation setup are detailed in Table 3 and Figure 13.

Table 3 Specification of the samples, obstacles and the instrumentation setup.

<b>Sample A:</b>	Pipe thickness = 7mm Pipe inner diameter = 156mm Pipe outer diameter = 170mm Insulator = carbon steel / calcium silicate Insulator thickness = 40mm Diameter of pipe + insulation = 250mm
<b>Sample B:</b>	Pipe thickness = 6.46mm Pipe inner diameter = 101.65mm Pipe outer diameter = 115mm Insulator = carbon steel / calcium silicate Insulator thickness = 25mm Diameter of pipe + insulation = 165mm
<b>Obstacles placed into</b>	Polypropylene log diameter = 136mm Concrete log diameter = 100mm

<b>pipeline:</b>	Hollow polypropylene log:- inner diameter = 25mm outer diameter = 105mm thickness = 40mm Hollow wax log:- inner diameter = 40mm outer diameter = 100mm thickness = 40mm
<b>Initial setup:</b>	Ratemeter HV dial setting = 2.6kV Ratemeter threshold = 1 Source = Cs-137, 2.8mCi Number of readings taken = 60 for sample A, 40 for sample B Stepper motor interval = 5mm Count period = 12 seconds



Figure 13: Left to right, Polypropylene log, concrete log, hollow polypropylene log, hollow wax log.

From the graphs in Figures 14-22, the thickness of the pipe, insulation and diameter of the obstacles can be predicted accurately based on the increase and the decrease of the intensity counts. As the gamma irradiates the object under test, a portion of the rays were absorbing by the object and the rest were allowing to pass through. Data obtained was in the form of intensity after traversing the medium. 60 readings were taken at every 5mm for Sample A and 40 readings were taken at every 5mm for Sample B.

The graphs indicate very significant changes in the intensity when there are changes in density of the objects obstructing the transmitted rays and when the total volume of material to be traversed increases or decreases. The system is able to perform object detection for any object located in the pipeline or on the outer surface of the pipeline as long as it is in the path of the incident beam and limited to static objects.



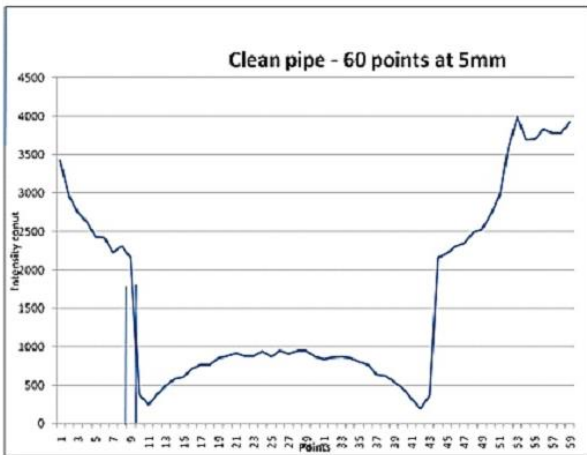


Figure 14: Sample A clean pipe profile

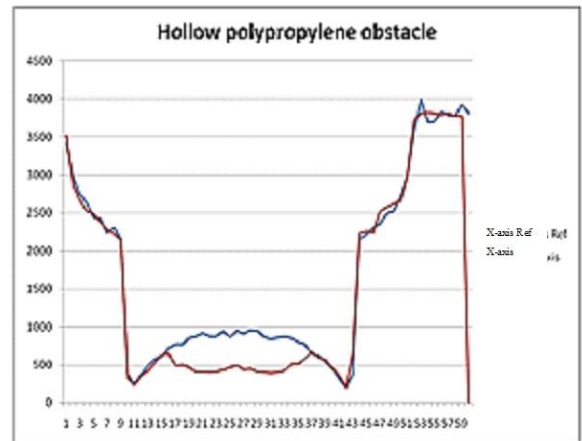


Figure 17: Sample A pipe profile with hollow polypropylene obstacle inserted.

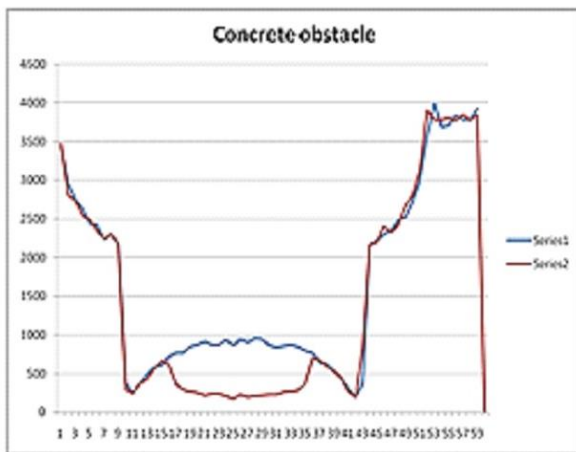


Figure 15: Sample A pipe profile with solid concrete obstacle inserted.

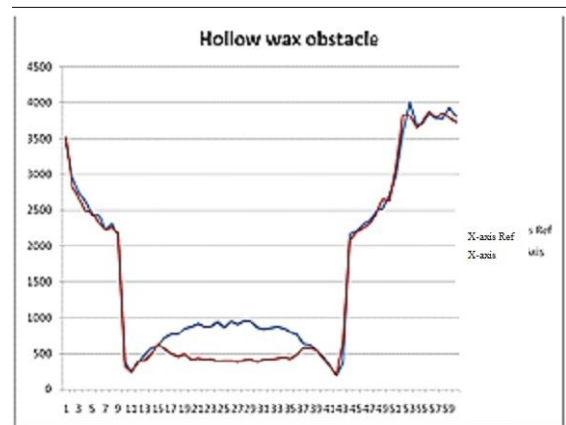


Figure 18: Sample A pipe profile with hollow wax obstacle inserted.

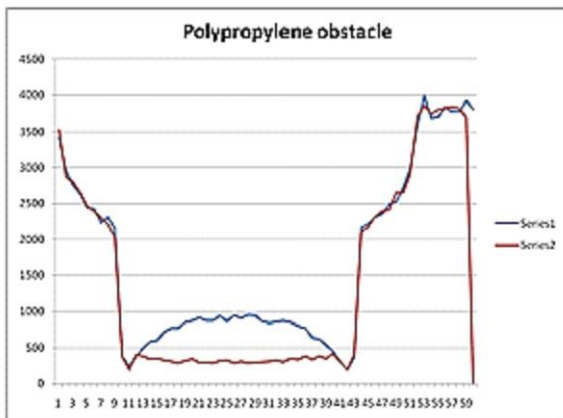


Figure 16: Sample A pipe profile with solid polypropylene obstacle inserted.

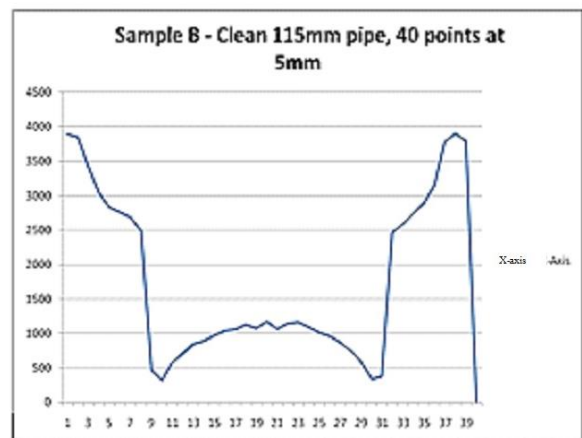


Figure 19: Sample B clean pipe profile.

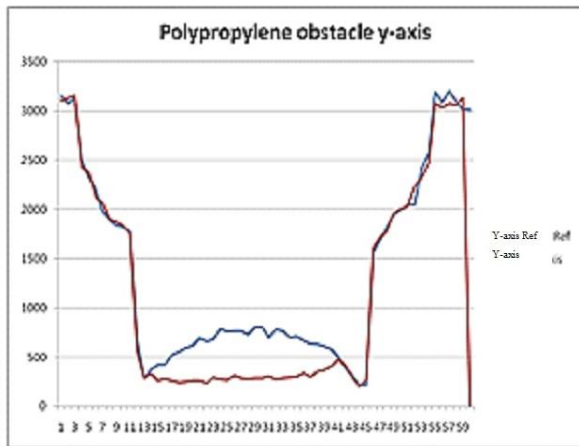


Figure 20: Sample B pipe profile with solid polypropylene obstacle inserted.

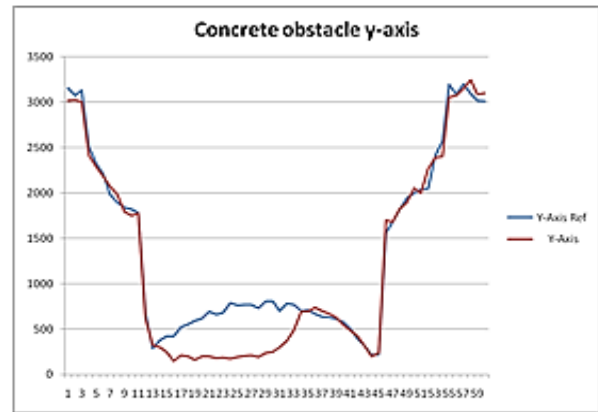


Figure 23: Sample B pipe profile with solid concrete obstacle inserted

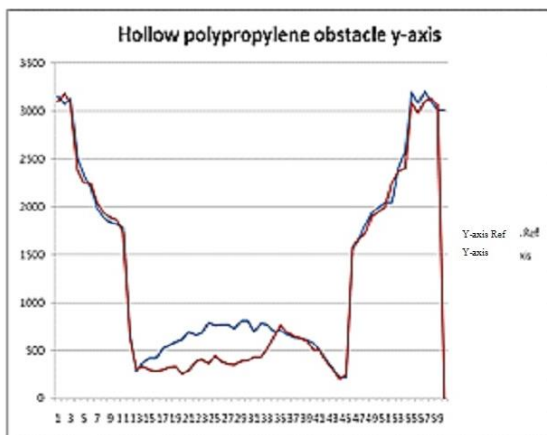


Figure 21: Sample B pipe profile with hollow polypropylene obstacle inserted.

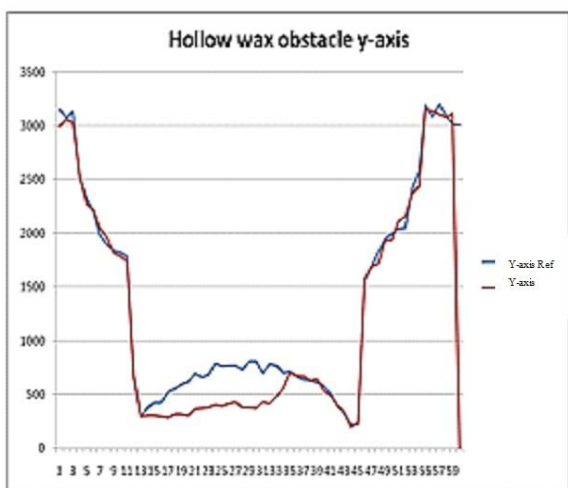


Figure 22: Sample B pipe profile with hollow wax obstacle inserted.

Figure 24 shows how the line profile produced along the x-axis and the y-axis profiles can be used to verify actual pipe dimension.

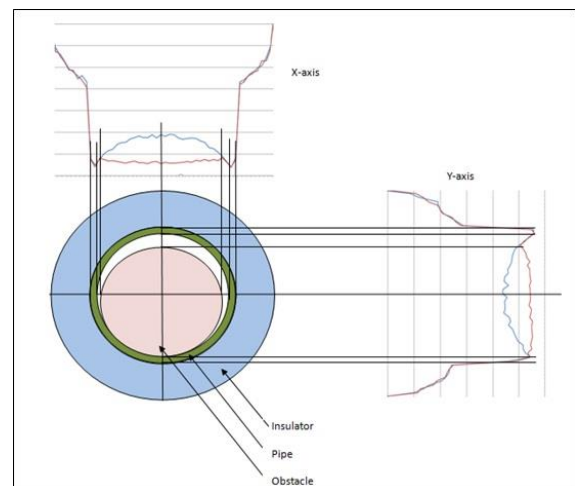


Figure 24: Using x-axis and y-axis profiles to reconstruct actual pipeline.

The intensity profiles of a clean pipe, Figure 14, and a pipe with a concrete piece placed in its cavity, Figure 15, are compared. In Figure 14, the first gradual drop in the intensity readings (points 0-9) indicate that the incident beam has met with an obstruction and has thus been partially absorbed. This material is the insulator. The decrease in the intensity is due to the increase in the volume of material that has to be traversed by the incident beam. Following this gradual drop, a significant drop in the intensity readings is noted (points 9-11) an is indication of the presence of a denser material, in this case it is the pipeline with

insulation. In Figure 15, a ‘crater’ is noted in the centre of the intensity profile. The peaks of the crater indicate the combined density of the pipeline and insulation at those points is lower than at the centre. The centre area having the combined density of the pipeline, insulation and concrete piece has the highest density and is indicated by the lowest intensity reading. With only one projection data set, we can only predict the presence of an object that has a width which is less than the diameter of the pipeline in the cavity of the larger pipeline. There is not much indication of the actual shape that can be predicted from one projection. However to illustrate the explanation above, an object with a circular crosssection is shown to sit in the cavity of the pipeline as shown in Figure 25.

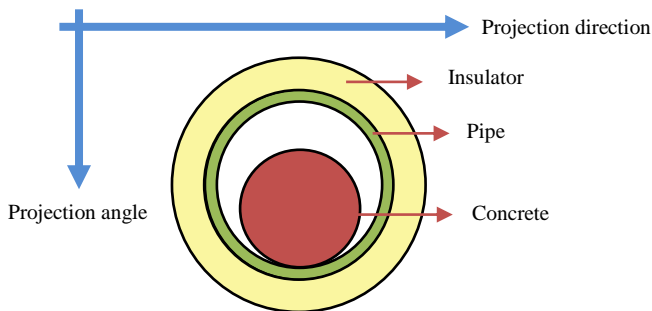


Figure 25: Predicted object placement based on intensity profile from one projection

The intensity profiles of a clean pipe, Figure 14, and a pipe with a hollow polypropylene piece placed in its cavity, Figure 17, are compared. Similarly for Figure 14, the first gradual drop in the intensity readings (points 0-9) indicate that the incident beam has met with an obstruction and has thus been partially absorbed. In Figure 17, a ‘crater’ is noted in the centre of the intensity profile. In comparison to the intensity profile for Figure 15, the intensity profile for this projection has a slight peak right at the centre of the profile. This indicates that the combined density of the object, pipeline and insulation at that central point has suddenly decreased causing the intensity to peak slightly. These conditions imply the possibility that the object within the pipeline has a cavity within it. With only one projection data set,

we can only predict the presence of an object that has a width which is less than the diameter of the pipeline and has a cavity sitting in the larger pipeline. There is not much indication of the actual shape that can be confirmed from one projection however the predicted shape is shown in the Figure 26.

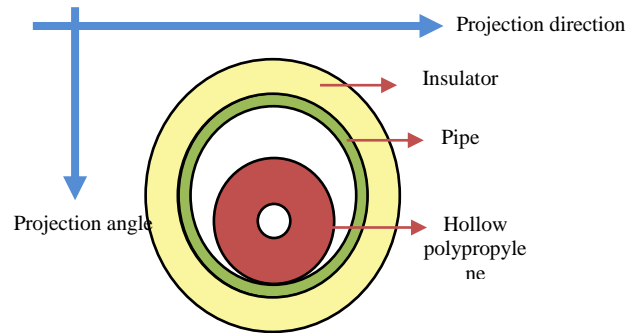


Figure 26: Predicted object placement based on intensity profile from one projection

The x-axis and the y-axis measurements correspond exactly to the pipe’s physical measurement when the points are extrapolated. The comparison between actual dimension of the objects under test and the dimension based on the intensity profiles is tabulated in Table 4. The actual pipe dimensions were measured using vernier calipers while the diameter from the graphs were obtained by multiplying each division by the 5mm, which was the interval spacing between each measurement point. The slight differences between the actual pipe at the graphed data was due to the distance between each measurement. By reducing the interval between measurements from 5 mm to 3 mm, thus increasing the sampling points, a more accurate representation of the pipe can be achieved.

Table 4 Comparison between actual dimension of the objects under test and the dimension based on the intensity profiles.

Sample	Actual dimension	Profile	Error (%)
A	Thickness = 7mm Inner diameter = 156mm Outer diameter = 170mm	<b>Referring to Figure 14</b>	
		Pipe thickness: 1.5 points x 5mm = 7.5 mm	7.14%
		Pipe inner diameter: 31 points x 5mm = 155mm	0.64%
		Pipe outer diameter: 34x 5mm = 170 mm	0%
	<b>Concrete log</b> diameter = 100mm	<b>Referring to Figure 15</b>	
		20 points x 5mm = 100mm	0%
	<b>Polypropylene log</b> diameter = 136mm	<b>Referring to Figure 16</b>	
		28 points x 5mm = 140mm	2.94%
	<b>Hollow polypropylene log</b> inner diameter = 25mm outer diameter = 105mm	<b>Referring to Figure 17</b>	
		Inner diameter: 5.5 points x 5mm = 27.5 mm	10%
	<b>Hollow wax log</b> inner diameter = 40mm outer diameter = 100mm	Outer diameter: 21.5 points x 5mm = 107.5 mm	2.38%
		<b>Referring to Figure 18</b>	
Inner diameter: 7.5 points x 5mm = 37.5 mm		6.25%	
	Outer diameter: 22 points x 5mm = 110	10%	

		mm	
B	Pipe thickness = 6.46mm Pipe inner diameter = 101.65mm Pipe outer diameter = 115mm	<b>Referring to Figure 19</b>	
		Pipe thickness: 1 point x 5mm = 5 mm	11.06%
		Pipe inner diameter: 20 points x 5mm = 100mm	1.62%
	<b>Polypropylene log</b> diameter = 136mm	Pipe outer diameter: 22 x 5mm = 110 mm	4.37%
		<b>Referring to Figure 20</b>	
	<b>Hollow polypropylene log</b> inner diameter = 25mm outer diameter = 105mm	Diameter: 27 points x 5mm = 135mm	0.74%
		<b>Referring to Figure 21</b>	
	<b>Hollow wax log</b> inner diameter = 40mm outer diameter = 100mm	Inner diameter: 5 points x 5mm = 25 mm	0%
		Outer diameter: 22 points x 5mm = 110 mm	4.76%
	<b>Hollow wax log</b> inner diameter = 40mm outer diameter = 100mm	<b>Referring to Figure 22</b>	
		Inner diameter: 8 points x 5mm = 40 mm	0%
	Concrete log Diameter = 100mm	Outer diameter: 21 points x 5mm = 105 mm	5%
<b>Referring to Figure 23</b>			
	Diameter :20 points x 5mm = 100mm	0%	

#### 4. Conclusion

Based on the experimental results, it was found that the system can successfully detect objects having a variety of sizes. Objects such as polypropylene logs, concrete logs, hollow

polypropylene logs and wax logs were placed into the cavity of the pipeline under test. These objects were of a different density from the pipeline. The system was able to achieve an average accuracy of 96.283% when a comparison was done between actual dimension of the objects under test and the dimension based on the intensity profiles. The intensity profiles obtained reflect the dimension and position very accurately regardless of the shape, size or density.

A stability test was performed using the developed gamma-ray tomography system to determine the most suitable operating voltage range (HV) for a scintillation detector. The chi-square values obtained for each HV setting fell in the valid range hence it can be concluded that these HV values obtained experimentally for each respective detector was its most suitable operating voltage, at which point readings obtained were stable and dependable.

From the results analysis, the line profile obtained using the intensity plot method will not be able to pinpoint the specific location and severity of any defects since its range is only at one projection angle. However it serves to inform the engineer about the possibility of a defect in the pipeline under test since the area with defects will have an intensity profile which has deviations from the intensity profile of a good pipeline.

## References

- [1] Beck, M. and Williams, R. (1996). Process tomography: a European innovation and its applications. *Measurement Science and Technology*, 7(3), pp.215-224.
- [2] Dyakowski, T. and Jaworski, A. (2003). Non-Invasive Process Imaging – Principles and Applications of Industrial Process Tomography. *Chemical Engineering & Technology*, 26(6), pp.697-706.
- [3] International Atomic Energy Agency (IAEA), IAEA-TECDOC-1589-Industrial Process Gamma Tomography, *Final report of a coordinated research project*, 2008, p. 3.
- [4] Kim, J., Jung, S., Moon, J., Kwon, T. and Cho, G. (2011). Monte Carlo Simulation for the Design of Industrial Gamma-ray Transmission Tomography. *Progress in Nuclear Science and Technology*, 1(0), pp.263-266.
- [5] Nelson, G. and Reilly, D., (1991). “Gamma-Ray Interactions with Matter”, in *Passive Non-destructive Analysis of Nuclear Materials*, Los Alamos National Laboratory, NUREG/CR-5550, LAUR-90-732, pp. 27-42.
- [6] Privitera, P. (2012). Detectors Fundamentals (for Dark Matter), Short Course for Museum and Planetarium Staff, Kavli Institute of Cosmological Physics, Univ. of Chicago.
- [7] Sampaio, R., Leite, A., (2008). Corrosion Under Insulation-Lessons Learned, Poster presented at *7th COFIC Process Safety Seminar*, The Dow Chemical Company, October 2008, Bahia, Brazil.
- [8] Wood, M. (2010). Corrosion Accidents in Refineries. Preliminary findings from a study of recent accidents in OECD/EU countries. Brussels, Belgium: JRC.
- [9] Twomey, M. (1997). Back to Basics - Inspection Techniques for Detecting Corrosion Under Insulation. *Materials Evaluation*, 55(2):129–132, February 1997.
- [10] Koch, G.H., Brongers, M.P.H., and Thompson, N.G., (2001), “Corrosion Costs and Preventive Strategies in the United States”, Publication No. FHWA-RD-01-156, CC Technologies Laboratories, Inc., Dublin, Ohio.
- [11] LUDLUM Model 2200 Scaler Ratemeter manual, Ludlum Measurements Inc., 2016